Spontaneous and Selective Macrocyclization in Nitroaldol Reaction Systems

Yunchuan Qi,[1] Mubarak Ayinla,[1] Stephen Clifford,[1] and Olof Ramström*[1,2]

[1]Department of Chemistry, University of Massachusetts Lowell, One University Ave., Lowell, MA 01854, USA; Email: olof_ramstrom@uml.edu; [2]Department of Chemistry and Biomedical Sciences, Linnaeus University, SE-39182 Kalmar, Sweden

Abstract

Through a dynamic polymerization and self-sorting process, a range of lowellane macrocycles have been efficiently generated in nitroaldol systems composed of aromatic dialdehydes and aliphatic or aromatic dinitroalkanes. All identified macrocycles show a composition of two repeating units, resulting in tetra-β-nitroalcohols of different structures. The effects of building block structure on the macrocyclization process have been demonstrated, and the influence from the solvent has been explored. In general, the formation of the lowellanes were amplified in response to phase-change effects, although solution-phase structures were in some cases favored.

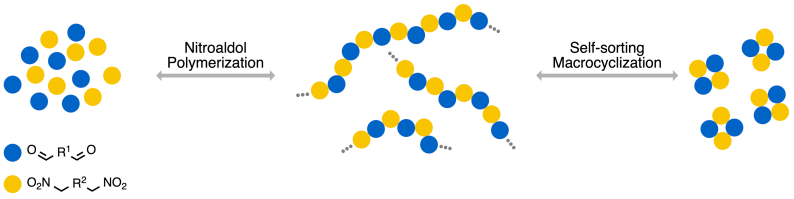

Introduction

Macrocycles are ubiquitous in nature and are vital to living organisms, such as macrocyclic peptides in cells and porphyrin structures in chlorophyll, hemes and vitamin B_{12}.[1–3] With cyclic structures of twelve or more atoms, macrocycles experience a restricted conformational space, while exhibiting rich functionalities.[4,5] Therefore, macrocycles have been in the focus of scientific research, especially in supramolecular chemistry and medicinal chemistry, for many decades.[4,6–8] Occasionally inspired by nature, a large variety of macrocycles have been synthesized, such as crown ethers,[9–13], cyclodextrins,[14–18] pillararenes,[19–23] cucurbiturils,[24–28] calixarenes,[29–33] and molecular cages.[34–38] Furthermore, macrocycles are part of rotaxanes and catenanes,[39–46] and are often used as components in molecular machines.[47,48] Due to their large cavities and rich binding sites, macrocycles are excellent scaffolds for noncovalent interactions, and have thus been extensively studied in supramolecular chemistry.[6,49] Moreover, many pharmaceuticals, naturally occurring or synthetic, have incorporated large cyclic structures, which makes macrocycles one of the key interests in drug discovery.[5,7,8] Therefore, it is of great importance to expand the collection of macrocycles and explore their potential applications.

Conventionally, macrocycle preparation often requires a judicious design of the synthesis route, although templates can be used to assist the cyclization through noncovalent interactions.[4,49–51] However, with the more recent upsurge in dynamic covalent chemistry applied to polymers, the spontaneous transition from dynamic covalent polymers (dynamers) to macrocycles under thermodynamic control has been observed in many systems,[52–54] such as imine and hydrazone formation/exchange,[55,56] alkene and alkyne metatheses,[35,57,58] disulfide formation/exchange,[59–61], amide formation,[62] and the nitroaldol reaction.[63] In principle, macrocycles can be designed and synthesized by selecting a specific set of monomers and controlling the reaction conditions in a dynamerization system. Self-sorting and error-c-

orrection effects may assist in the formation of specific cyclic structures without human intervention, provided that the desired macrocycles are thermodynamically favored.[52–54] This dynamic macrocyclization offers a new approach to constructing macrocycles with relative ease, compared to traditional methods, and can further promote the discovery of new applications of macrocyclic systems.

In our previous work, we described the first transformation of linear dynamers to macrocycles in a nitroaldol reaction system.[63] The resulting tetra-β-nitroalcohol macrocycles, or *lowellanes*, were formed through depolymerization of longer dynamer chains, providing a clear example of a ring-chain-type polymerization process. The resulting lowellane macrocycles have unique properties that make them interesting for further development and application, potentially also for biomedical purposes.[64] Therefore, it is of importance to expand the scope and explore the nature of this type of nitroaldol macrocyclization processes. Hence, in this study, a range of new nitroaldol dynamerization systems, potentially able to produce macrocycles, were investigated. The reactions of three aromatic dialdehydes with eleven dinitro-compounds (aliphatic and aromatic) were explored, where several new macrocyclic species were isolated and identified.

Results and Discussion

In our previous study, we demonstrated the dynamic polymerization and macrocyclization of 2,6-pyridinedicarboxaldehyde (**A1**) with α,ω-dinitroalkanes (**N1**).[63] To expand the macrocycle scope, dialdehyde **A1** and two other aromatic dialdehydes, 2,5-furandicarboxaldehyde (**A2**) and 1,10-phenanthroline-2,9-dicarbaldehyde (**A3**), were chosen as dialdehyde building blocks due to their electrophilic nature, which promotes the efficient formation of nitroaldol adducts. For the dinitroalkane blocks, eight aliphatic dinitroalkanes, including 1,3-dinitropropane (**N1a**), 1,4-dinitrobutane (**N1b**), 1,5-dinitropentane (**N1c**), 1,6-dinitrohexane (**N1d**), 1,7-dinitroheptane (**N1e**), 1,8-dinitrooctane (**N1f**), 1,9-dinitrononane (**N1g**), and 1,10-dinitrodecane (**N1h**) as well as their aromatic analogs, *i.e.*, 1,2-bis(nitromethyl)benzene (**N2o**), 1,4-bis(nitromethyl)benzene (**N2p**) and 1,3-bis(nitromethyl)benzene (**N2m**), were employed in the reactions. In addition, several polar organic solvents (acetonitrile, DMSO, methanol) were explored to evaluate the solubility effects, while triethylamine was generally used as the catalyst due to its high efficiency in the nitroaldol reaction.[63,65,66] Thus, the nitroaldol systems consisting of combinations of these building blocks interacting under different conditions were explored (**Figure 1**).

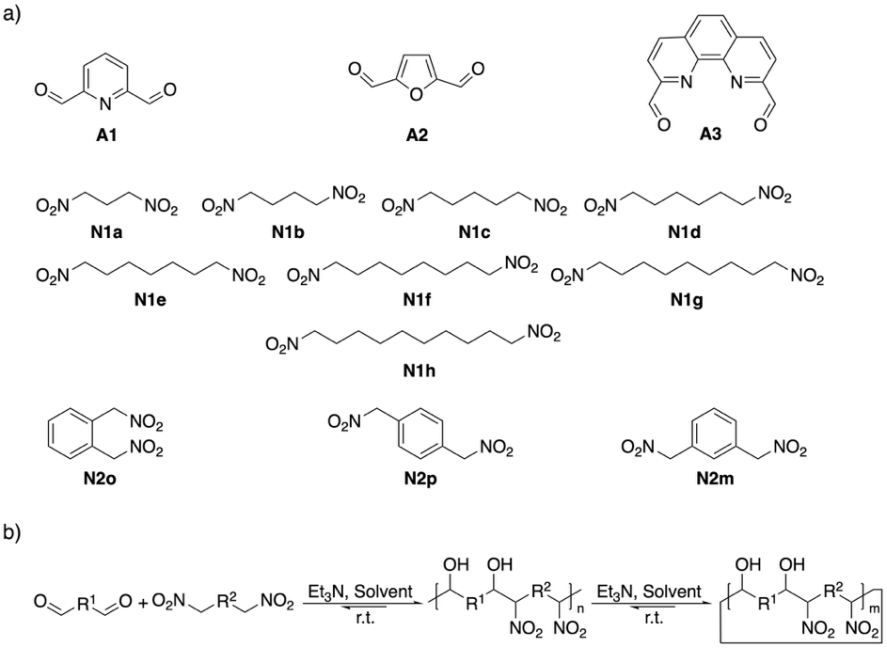

Figure 1: *a) Building blocks used in this study; b) general scheme of nitroaldol macrocyclization.*

The combination of dialdehyde **A1** and different dinitroalkanes (**N1a**–**N1h**) yielded several lowellane macrocycles in acetonitrile.[63] Therefore, by replacing the aliphatic dinitroalkanes with their aromatic analogs, the reactions between compound **A1** and the bis(dinitromethyl)benzenes (**N2o**, **N2m**, **N2p**) in acetonitrile were first carried out. Clear solutions were initially formed in all reactions, but a large amount of precipitate started to form in the solution of the reaction between dialdehyde **A1** and bis(nitromethyl)benzene **N2p** within 20 minutes after the base was added. ^{1}H-NMR analysis of the precipitate exhibited features of an aromatic β-nitroalcohol without any peaks corresponding to the protons from the aldehyde or nitromethyl groups (**Figure 2**c), indicating a full conversion of the starting materials. By consequence, the product structure should have a cyclic structure in order to satisfy the NMR results, and MS analysis also revealed that the compound had a molecular weight of the exact sum of two **A1** and two **N2p** moieties (Figure S21). Hence, the product from the reaction between dialdehyde **A1** and bis(nitromethyl)benzene **N2p** was a tetra-β-nitroalcohol consisting of two repeating units (**M1**, **Figure 2**a), which thus added a new member to the lowellane family.[63] In addition, 1D NOE analysis of lowellane **M1** revealed a nuclear Overhauser effect between the pyridine protons (b-H) and the protons on the benzene moiety (c-H) (**Figure 2**b), indicating that the two aromatic rings were in relatively close proximity, and that the macrocycle would have a comparatively compact structure.

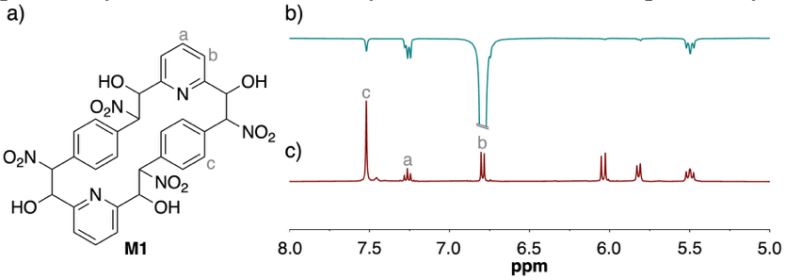

Figure 2: *a) Structure; b) 1D NOE NMR spectrum (Excitation: 6.8 ppm); c) ^{1}H-NMR spectrum, of lowellane **M1** (400 MHz, DMSO-d_6).*

However, the reactions involving dialdehyde **A1** and bis(nitromethyl)benzenes **N2o** or **N2m** did not yield any precipitates and ^{1}H-NMR spectroscopy showed broad but not smooth

peaks, indicating a lack of extensive polymerization (Figure S1). This could be caused by the fact that the *para*-disubstituted bis(nitromethyl)benzene would lead to a less strained geometry, in the formation of macrocycles with 2,6-pyridinedicarboxaldehyde, than the corresponding *ortho*- or *meta*-substituted dinitroalkanes.

2,5-furandicarboxaldehyde (**A2**) was then applied in the reactions with the eight α,ω-dinitroalkanes (**N1a**–**N1h**) in acetonitrile. After 24 h, ^{1}H-NMR analysis revealed that a considerable amount of aldehyde groups and nitroalkanes were still present in the solutions (Figure S2), indicating less prominent oligomerization. This could be reflective of the weaker electron-withdrawing ability of furan compared to the pyridine ring, which then leads to the lower reactivity of dialdehyde **A2** compared to compound **A1** in the nitroaldol reaction.[67]

However, somewhat surprisingly, solids started to precipitate out from five of the eight solutions after 3-7 days. The precipitates were collected and analyzed, and the results revealed the formation of five new lowellanes (**M2**-**M6**, **Figure 3**, Figure S22–Figure S36). This demonstrates that even without efficient polymerization, the systems were able to generate macrocycles, possibly driven by the limited solubility of these macrocycles in acetonitrile, which worked as a stimulus to induce the formation of these cyclic molecules.[68]

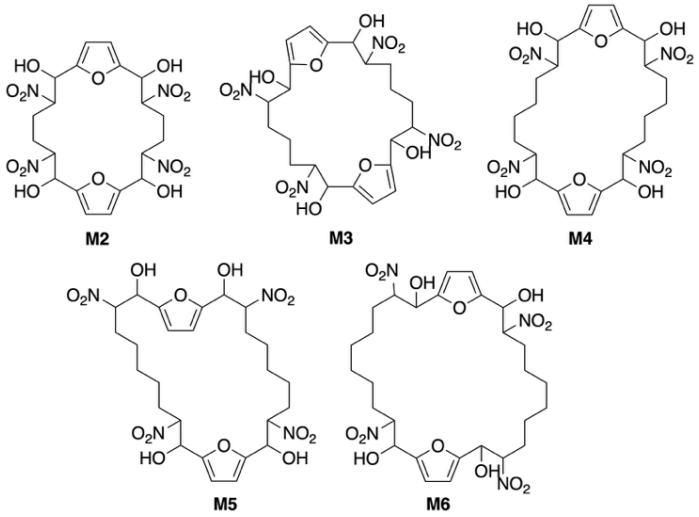

Figure 3: *Macrocycles **M2**–**M6** formed in the reactions between dialdehyde **A2** and dinitroalkanes **N1b**–**N1f** in acetonitrile.*

To promote the polymerization in the **A2**/**N1** system and explore the effects of the solvents, acetonitrile was replaced by DMSO due to the higher solubility of the nitroaldol adducts, which would repress the precipitation-driven depolymerization. Stable solutions were formed in all reactions, except that precipitation still occurred in the reaction between dialdehyde **A2** and dinitrobutane (**N1b**). Characterization results of the precipitate revealed that it was composed of macrocycle **M2** (Figure S37–Figure S39), which could be caused by its low solubility even in DMSO. Upon closer examination, it was found that, although lowellane **M2** obtained from two different solvents had the same molecular weight, their ^{1}H-NMR spectra showed peaks at the same chemical shifts but of different intensities (**Figure 4**). Since lowellane **M2** has eight chiral centers, these results indicate a different distribution of stereoisomers, which could be reflective of the different macrocyclization environments.

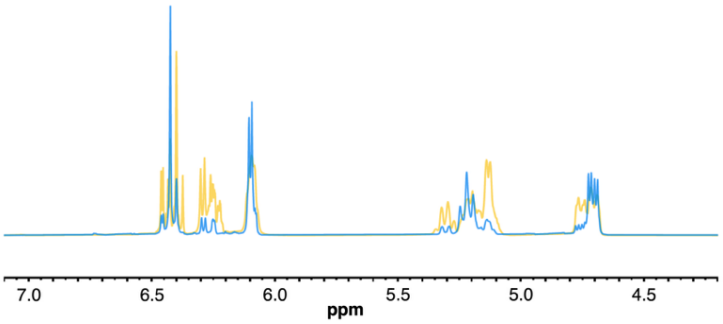

Figure 4: *^{1}H-NMR spectra of lowellane **M2** from acetonitrile (blue) and DMSO (yellow) (400 MHz, DMSO-d_6).*

In contrast, the combination of dialdehyde **A2** and dinitropropane (**N1a**) did not produce macrocycles or polymers due to stability issues of the formed nitroalcohols.[63,65] However, broad peaks were exhibited in the ^{1}H-NMR spectra of the solutions of dialdehyde **A2** and dinitroalkanes **N1c**–**N1h** (Figure S3), indicating a more pronounced polymerization process than the corresponding reactions in acetonitrile. Gel permeation chromatography (GPC) showed that oligomer peaks were only detected in the reactions involving longer dinitroalkanes **N1d**–**N1h**, and the number average molecular weights M_n ranged from 2200–3500 and the degrees of polymerization varied from 7 to 10 (**Table 1**). These results demonstrate that the systems undergo good oligomerization but less macrocyclization due to the high solubility of those macrocycles in DMSO. Without precipitation as the driving force, the dynamer-macrocycle transition was in these cases hampered.

Table 1: *GPC data of oligomers in the reactions of **A2** and **N1** in DMSO.*

Reaction	M_n (g/mol)	M_w (g/mol)	M_z (g/mol)	$Đ$	DP
A2/N1d	2200	2400	2500	1.1	7
A2/N1e	2400	2600	2800	1.1	8
A2/N1f	2800	3300	4000	1.2	9
A2/N1g	3000	3600	4300	1.2	9
A2/N1h	3500	4300	5100	1.2	10

$Đ$: polydispersity index; DP: degree of polymerization

Interestingly, the product from the solution of dialdehyde **A2** and 1,5-dinitropentane (**N1c**) in DMSO showed no polymer peaks by GPC, but was later identified to be macrocycle **M3** (Figure S40–Figure S42). This indicates that macrocycles can be formed to a high degree in the reaction even without precipitation, and that this structure was thermodynamically favored in the system.

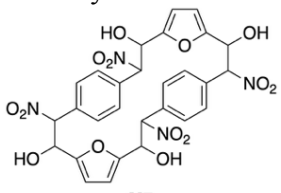

M7

Figure 5: *Structure of lowellane **M7**.*

In light of the efficient macrocyclization of dialdehyde **A1** and the *para*-disubstituted aromatic structure **N2p**, the reaction between compounds **A2** and **N2p** in acetonitrile was next investigated. As expected, a yellow precipitate, falling out from the solution after 24 h, was revealed to be lowellane **M7** (**Figure 5**, Figure S43–Figure S45). The similarity between **M1** and **M7** indicates that the nitroaldol macrocyclization can be designed and predicted if the starting materials and reaction conditions are carefully selected.

To explore the macrocyclization in systems with larger aromatic moieties, 1,10-

phenanthroline-2,9-dicarbaldehyde (**A3**) was chosen since it has fused pyridine rings and similar reactivity as dialdehyde **A1** in the nitroaldol reaction. However, due to the strong π–π stacking effect of phenanthroline rings,[69] dialdehyde **A3** shows very low solubility in many common solvents, thereby hampering its application. To address this challenge, a secondary dynamic covalent reaction was adopted, and it was found that the phenanthroline aldehyde could be sufficiently dissolved in NEt_3-containing methanol through reversible hemiacetal formation (**Figure 6**, Figure S5). Thus, instead of using compound **A3** in its pure aldehyde form, the hemiacetals would serve as an aldehyde reservoir for the nitroaldol reaction.

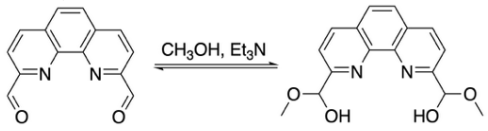

Figure 6: *Hemiacetal formation in the reaction of phenanthroline dialdehyde **A3** with methanol in the presence of Et_3N.*

The reaction of phenanthroline dialdehyde **A3** in basic methanol solution with dinitroalkane **N1d** was first carried out to test whether the hemiacetal formation was compatible with the nitroaldol reaction. Although a clear solution was initially formed, precipitates started to form within minutes. ^{1}H-NMR and GPC results revealed that the product was a nitroalcohol oligomer with an average of five repeating units (Figure S6–Figure S7). This was assumed to be caused by the low solubility of the phenanthroline-based nitroalcohols in methanol, leading to precipitation and insufficient time for the transformation of the dynamers to macrocycles. To address this issue, instead of only using methanol, mixed solvents were applied in the reactions to increase the solubility of the oligomers based on dialdehyde **A3**.

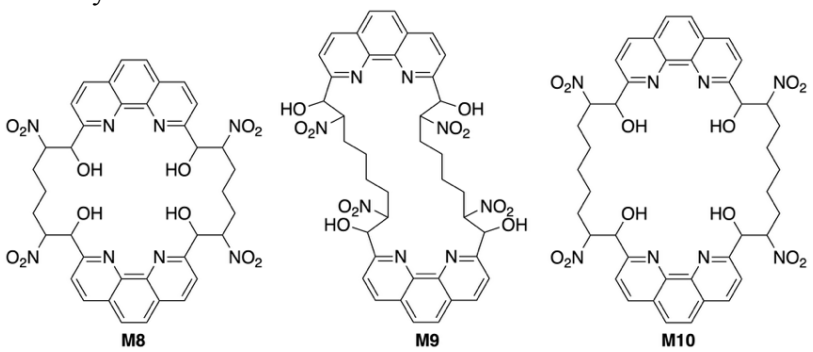

Figure 7: *Macrocycles formed in the reactions of **A3** with **N1**.*

In a mixture of methanol and acetonitrile, solutions of phenanthroline dialdehyde **A3** with dinitroalkanes **N1a** and **N1b** did not lead to precipitation until after several hours, and the ^{1}H-NMR results showed that the solids were complex mixtures of nitroalcohols (Figure S8). On the other hand, in the reactions with compounds **N1c** and **N1d**, solids started to appear after 24 h, and further analyses revealed that these precipitates were composed of lowellanes **M8** and **M9** (Figure S46–Figure S51). Moreover, lowellane **M10** could also be identified in the reaction of dialdehyde **A3** with compound **N1e**, precipitating out from the mixed solvent of methanol and chloroform (Figure S52–Figure S54). In contrast, the reactions between compound **A3** and dinitroalkanes **N1f**–**N1h** remained in the solution state without any precipitation. These results demonstrate that the alkane chain length in the starting material, as well as the solvent, play important roles in determining if macrocyclization occurs in these nitroaldol reaction systems.

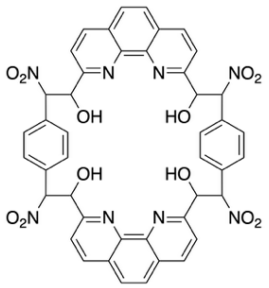

Figure 8: *Macrocycle **M11** formed in the reaction between dialdehyde **A3** and bis(nitromethyl)benzene **N2p**.*

To complete the series of combinations, the reaction between phenanthroline dialdehyde **A3** and bis(nitroaldol)benzene **N2p** was carried out in a mixture of methanol and acetonitrile. As predicted, a precipitate was again isolated from the solution, and the ^{1}H-NMR analysis of the product resulted in very broad signals with low resolution, indicative of strong π–π stacking (Figure S55). MS data revealed that the compound was composed of two of each starting material, implying formation of lowellane **M11** (**Figure 8**). These results again demonstrate the excellent performance of 1,4-bis(nitromethyl)benzene in the macrocyclization with dialdehydes.

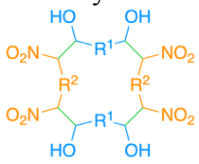

Figure 9: *General structure of known lowellanes.*

The previously reported lowellanes,[63] and those synthesized in this study are all composed of two of their respective repeating units. In comparison with oligomerization/polymerization, macrocyclization is a unimolecular process that becomes favored under dilute conditions when the concentration of monomer units is low.[53,54,70] For dynamic covalent polymers, the thermodynamics of the system also comes into play, governed by the respective equilibria of the many connections taking place. Furthermore, due to the abundant reversible linkages in larger dynamers, bond-breaking events happen more frequently. As a result, the degrees of polymerization are typically low in such systems.

As shown in our previous study,[63] a ring-chain-type polymerization process can take place in nitroaldol polymerization systems, and the systems are composed of both macrocycles and oligomers to different degrees. Although macrocycles of different size in principle can be formed, smaller cycles form easier due to proximity effects, provided the macrocycle structure remains unstrained, and are therefore favored in dynamer systems at equilibrium.[53,54,70] In our case, the associated phase-change of certain macrocycles play an important role in determining the distribution of the adducts. Due to the low solubility of the two-unit macrocycles in organic solvents, their precipitation perturbs the overall equilibria and amplifies the selective formation of these lowellanes.

Conclusions

In summary, spontaneous and selective macrocyclization has been realized in several nitroaldol reaction systems. Eleven new lowellane macrocycles, each composed of two repeating units, have been identified. The effects of starting materials of different structure, as well as different solvents and solvent combinations, have been investigated, in general leading to efficient macrocycle formation. In most cases, precipitation-driven depolymerization and formation of the resulting lowellane macrocycles were observed, although thermodynamically favored macrocycles were also formed in solution in some cases. These results demonstrate

the high dynamicity of the nitroaldol reaction and the feasibility and propensity of such systems to lead to specific, new macrocycles of predicted structure. This work provides a new approach to building discrete cyclic structures and the resulting nitroalcohol macrocycles composed of aromatic moieties have the potential to be applied in the construction of intricate molecular architectures and exploring supramolecular interactions. Furthermore, the intriguing properties of lowellanes and their derivatives augurs for various applications in chemistry and related areas.

Acknowledgments

Y.Q. thanks the China Scholarship Council for a special scholarship award. We thank Wendy Gavin for technical support. Mass spectral data were obtained at the University of Massachusetts Mass Spectrometry Core Facility, RRID:SCR_019063. We thank Dr. Steve Eyles and Dr. Cedric Bobst for their kind help on HRMS measurements.

References

(1) Park, J. M.; Hong, K.-I.; Lee, H.; Jang, W.-D. *Acc. Chem. Res.* **2021**, *54* (9), 2249–2260.

(2) Smolyar, I. V.; Yudin, A. K.; Nenajdenko, V. G. *Chem. Rev.* **2019**, *119* (17), 10032–10240.

(3) Vinogradov, A. A.; Yin, Y.; Suga, H. *J. Am. Chem. Soc.* **2019**, *141* (10), 4167–4181.

(4) K. Yudin, A. *Chem. Sci.* **2015**, *6* (1), 30–49.

(5) Heinis, C. *Nat. Chem. Biol.* **2014**, *10* (9), 696–698.

(6) He, Q.; Vargas-Zúñiga, G. I.; Kim, S. H.; Kim, S. K.; Sessler, J. L. *Chem. Rev.* **2019**, *119* (17), 9753–9835.

(7) Marsault, E.; Peterson, M. L. *J. Med. Chem.* **2011**, *54* (7), 1961–2004.

(8) Driggers, E. M.; Hale, S. P.; Lee, J.; Terrett, N. K. *Nat. Rev. Drug Discovery* **2008**, *7* (7), 608–624.

(9) Zhang, Y.-F.; Di, F.-F.; Li, P.-F.; Xiong, R.-G. *Chem. Eur. J.* **2022**, *28* (5), e202102990.

(10) Xia, Y.; Song, Z.; Tan, Z.; Xue, T.; Wei, S.; Zhu, L.; Yang, Y.; Fu, H.; Jiang, Y.; Lin, Y.; Lu, Y.; Ferguson, A. L.; Cheng, J. *Nat. Commun.* **2021**, *12* (1), 732.

(11) Yoo, C.; M. Dodge, H.; M. Miller, A. J. *Chem. Commun.* **2019**, *55* (35), 5047–5059.

(12) Gokel, G. W.; Leevy, W. M.; Weber, M. E. *Chem. Rev.* **2004**, *104* (5), 2723–2750.

(13) Pedersen, C. J. *Angew. Chem. Int. Ed. Engl.* **1988**, *27* (8), 1021–1027.

(14) Hanayama, H.; Yamada, J.; Tomotsuka, I.; Harano, K.; Nakamura, E. *J. Am. Chem. Soc.* **2021**, *143* (15), 5786–5792.

(15) Achkar, T. E.; Moufawad, T.; Ruellan, S.; Landy, D.; Greige-Gerges, H.; Fourmentin, S. *Chem. Commun.* **2020**, *56* (23), 3385–3388.

(16) Jones, S. T.; Cagno, V.; Janeček, M.; Ortiz, D.; Gasilova, N.; Piret, J.; Gasbarri, M.; Constant, D. A.; Han, Y.; Vuković, L.; Král, P.; Kaiser, L.; Huang, S.; Constant, S.; Kirkegaard, K.; Boivin, G.; Stellacci, F.; Tapparel, C. *Sci. Adv.* **2020**, *6* (5), eaax9318.

(17) Jin, H.; Yang, L.; Ahonen, M. J. R.; Schoenfisch, M. H. *J. Am. Chem. Soc.* **2018**, *140* (43), 14178–14184.

(18) Crini, G. *Chem. Rev.* **2014**, *114* (21), 10940–10975.

(19) Sheng, X.; Li, E.; Zhou, Y.; Zhao, R.; Zhu, W.; Huang, F. *J. Am. Chem. Soc.* **2020**, *142* (13), 6360–6364.

(20) Zhu, H.; Li, Q.; Gao, Z.; Wang, H.; Shi, B.; Wu, Y.; Shangguan, L.; Hong, X.; Wang, F.; Huang, F. *Angew. Chem. Int. Ed.* **2020**, *59* (27), 10868–10872.

(21) Jie, K.; Zhou, Y.; Li, E.; Huang, F. *Acc. Chem. Res.* **2018**, *51* (9), 2064–2072.

(22) Zhang, H.; Zhao, Y. *Chem. Eur. J.* **2013**, *19* (50), 16862–16879.

(23) Xue, M.; Yang, Y.; Chi, X.; Zhang, Z.; Huang, F. *Acc. Chem. Res.* **2012**, *45* (8), 1294–1308.

(24) Yu, H.-J.; Zhou, X.-L.; Dai, X.; Shen, F.-F.; Zhou, Q.; Zhang, Y.-M.; Xu, X.; Liu, Y. *Chem. Sci.* **2022**, *13* (27), 8187–8192.

(25) Liu, Y.-H.; Zhang, Y.-M.; Yu, H.-J.; Liu, Y. *Angew. Chem. Int. Ed.* **2021**, *60* (8), 3870–3880.

(26) Yang, X.; Wang, R.; Kermagoret, A.; Bardelang, D. *Angew. Chem. Int. Ed.* **2020**, *59* (48), 21280–21292.

(27) Barrow, S. J.; Kasera, S.; Rowland, M. J.; Barrio, J. del; Scherman, O. A. *Chem. Rev.* **2015**, *115* (22), 12320–12406.

(28) Freeman, W. A.; Mock, W. L.; Shih, N. Y. *J. Am. Chem. Soc.* **1981**, *103* (24), 7367–7368.

(29) Crowley, P. B. *Acc. Chem. Res.* **2022**, *55* (15), 2019–2032.

(30) Feng, H.-T.; Li, Y.; Duan, X.; Wang, X.; Qi, C.; Lam, J. W. Y.; Ding, D.; Tang, B. Z. *J. Am. Chem. Soc.* **2020**, *142* (37), 15966–15974.

(31) Schulz, M.; Gehl, A.; Schlenkrich, J.; Schulze, H. A.; Zimmermann, S.; Schaate, A. *Angew. Chem. Int. Ed.* **2018**, *57* (39), 12961–12965.

(32) Homden, D. M.; Redshaw, C. *Chem. Rev.* **2008**, *108* (12), 5086–5130.

(33) Böhmer, V. *Angew. Chem. Int. Ed. Engl.* **1995**, *34* (7), 713–745.

(34) Shan, Z.; Wu, X.; Xu, B.; Hong, Y.; Wu, M.; Wang, Y.; Nishiyama, Y.; Zhu, J.; Horike, S.; Kitagawa, S.; Zhang, G. *J. Am. Chem. Soc.* **2020**, *142* (51), 21279–21284.

(35) C. Pattillo, C.; S. Moore, J. *Chem. Sci.* **2019**, *10* (29), 7043–7048.

(36) Collins, M. S.; Phan, N.-M.; Zakharov, L. N.; Johnson, D. W. *Inorg. Chem.* **2018**, *57* (7), 3486–3496.

(37) Feng, H.-T.; Yuan, Y.-X.; Xiong, J.-B.; Zheng, Y.-S.; Tang, B. Z. *Chem. Soc. Rev.* **2018**, *47* (19), 7452–7476.

(38) Granzhan, A.; Riis-Johannessen, T.; Scopelliti, R.; Severin, K. *Angew. Chem. Int. Ed.* **2010**, *49* (32), 5515–5518.

(39) Wu, Y.; Guo, Q.-H.; Qiu, Y.; Weber, J. A.; Young, R. M.; Bancroft, L.; Jiao, Y.; Chen, H.; Song, B.; Liu, W.; Feng, Y.; Zhao, X.; Li, X.; Zhang, L.; Chen, X.-Y.; Li, H.; Wasielewski, M. R.; Stoddart, J. F. *Proc. Natl. Acad. Sci.* **2022**, *119* (12), e2118573119.

(40) Imayoshi, A.; Lakshmi, B. V.; Ueda, Y.; Yoshimura, T.; Matayoshi, A.; Furuta, T.; Kawabata, T. *Nat. Commun.* **2021**, *12* (1), 404.

(41) Kwamen, C.; Niemeyer, J. *Chem. Eur. J.* **2021**, *27* (1), 175–186.

(42) Li, P.; Xu, S.; Yu, C.; Li, Z.-Y.; Xu, J.; Li, Z.-M.; Zou, L.; Leng, X.; Gao, S.; Liu, Z.; Liu, X.; Zhang, S. *Angew. Chem. Int. Ed.* **2020**, *59* (18), 7113–7121.

(43) Rodrigues, R. D. S.; L. Marshall, D.; C. McMurtrie, J.; M. Mullen, K. *New J. Chem.* **2020**, *44* (26), 11231–11236.

(44) Mena-Hernando, S.; M. Pérez, E. *Chem. Soc. Rev.* **2019**, *48* (19), 5016–5032.

(45) Van Raden, J. M.; White, B. M.; Zakharov, L. N.; Jasti, R. *Angew. Chem. Int. Ed.* **2019**, *58* (22), 7341–7345.

(46) Jinks, M. A.; Juan, A. de; Denis, M.; Fletcher, C. J.; Galli, M.; Jamieson, E. M. G.; Modicom, F.; Zhang, Z.; Goldup, S. M. *Angew. Chem. Int. Ed.* **2018**, *57* (45), 14806–14810.

(47) Sauvage, J.-P. *Angew. Chem. Int. Ed.* **2017**, *56* (37), 11080–11093.

(48) Stoddart, J. F. *Angew. Chem. Int. Ed.* **2017**, *56* (37), 11094–11125.

(49) Yu, J.; Qi, D.; Li, J. *Commun. Chem.* **2020**, *3* (1), 1–14.

(50) Mortensen, K. T.; Osberger, T. J.; King, T. A.; Sore, H. F.; Spring, D. R. *Chem. Rev.* **2019**, *119* (17), 10288–10317.

(51) Laughrey, Z. R.; Gibb, B. C. In *Templates in chemistry II: -/-*; Schalley, C. A., Vögtle, F., Dötz, K. H., Eds.; Springer Berlin Heidelberg: Berlin, Heidelberg, 2005; pp 67–125.

(52) Martí-Centelles, V. *Tetrahedron Lett.* **2022**, *93*, 153676.

(53) Aoki, D. *Polym. J.* **2021**, *53* (2), 257–269.

(54) Rowan, S. J.; Cantrill, S. J.; Cousins, G. R. L.; Sanders, J. K. M.; Stoddart, J. F. *Angew. Chem. Int. Ed.***2002**, 55.

(55) Zhang, Y.; Zheng, X.; Cao, N.; Yang, C.; Li, H. *Org. Lett.* **2018**, *20* (8), 2356–2359.

(56) Chavez, A. D.; Evans, A. M.; Flanders, N. C.; Bisbey, R. P.; Vitaku, E.; Chen, L. X.; Dichtel, W. R. *Chem. Eur. J.* **2018**, *24* (16), 3989–3993.

(57) Gross, D. E.; Moore, J. S. *Macromolecules* **2011**, *44* (10), 3685–3687.

(58) Zhang, W.; Brombosz, S. M.; Mendoza, J. L.; Moore, J. S. *J. Org. Chem.* **2005**, *70* (24), 10198–10201.

(59) Tsurumi, N.; Takashima, R.; Aoki, D.; Kuwata, S.; Otsuka, H. *Angew. Chem. Int. Ed.* **2020**, *59* (11), 4269–4273.

(60) Liu, Y.; Jia, Y.; Wu, Q.; Moore, J. S. *J. Am. Chem. Soc.* **2019**, *141* (43), 17075–17080.

(61) Pal, A.; Malakoutikhah, M.; Leonetti, G.; Tezcan, M.; Colomb-Delsuc, M.; Nguyen, V. D.; Gucht, J. van der; Otto, S. *Angew. Chem. Int. Ed.* **2015**, *54* (27), 7852–7856.

(62) Erguven, H.; Keyzer, E. N.; Arndtsen, B. A. *Chem. Eur. J.* **2020**, *26* (25), 5709–5716.

(63) Qi, Y.; Ramström, O. *Chem. Eur. J.* **2022**, *e202201863*.

(64) Zhang, Y.; Qi, Y.; Ulrich, S.; Barboiu, M.; Ramström, O. *Mater. Chem. Front.* **2020**, *4* (2), 489–506.

(65) Qi, Y.; Ayinla, M.; Sobkowicz, M. J.; Ramström, O. *Macromol. Rapid Commun.* **2023**, *44* (10), 2300011.

(66) Vongvilai, P.; Angelin, M.; Larsson, R.; Ramström, O. *Angew. Chem. Int. Ed.* **2007**, *46* (6), 948–950.

(67) Vongvilai, P.; Larsson, R.; Ramström, O. *Adv. Synth. Catal.* **2008**, *350* (3), 448–452.

(68) Angelin, M.; Vongvilai, P.; Fischer, A.; Ramström, O. *Eur. J. Org. Chem.* **2010**, *2010* (33), 6315–6318.

(69) Nisbet, M. L.; Wang, Y.; Poeppelmeier, K. R. *Cryst. Growth Des.* **2021**, *21* (1), 552–562.

(70) Greenlee, A. J.; Wendell, C. I.; Cencer, M. M.; Laffoon, S. D.; Moore, J. S. *Trends Chem.* **2020**, *2* (12), 1043–1051.